1981ApJ...247...52N

THE ASTROPHYSICAL JOURNAL 247:52–58, 1981 July 1
© 1981. The American Astronomical Society. All rights reserved. Printed in U.S.A.

HYDRODYNAMIC FORMATION OF TWIN-EXHAUST JETS

MICHAEL L. NORMAN
Department of Applied Science, University of California, Davis; and Lawrence Livermore Laboratory, University of California, Livermore

LARRY SMARR
Department of Astronomy, University of Illinois, Urbana,

JAMES R. WILSON
Lawrence Livermore Laboratory, University of California, Livermore

AND

MICHAEL D. SMITH
Department of Physics, University of Illinois, Urbana
Received 1980 July 7; accepted 1981 January 8

ABSTRACT

We perform a numerical study of the formation and stability of a Blandford-Rees (BR) twin exhaust jet. A de Laval nozzle is indeed created and stably maitained over a central luminosity range of ~ 40. However, the cavity-nozzle structure is compact and dominated by a central spherical shock unlike BR's original models. We find a new global Rayleigh-Taylor instability which limits the formation of high-luminosity jets. A useful formula is discovered for relating the jet luminosity to the internal energy of the confining cloud.

Subject headings: hydrodynamics — radio sources: general

I. INTRODUCTION

Jets have been observed in a wide variety of astronomical objects: quasars, radio galaxies, and SS 433. One of the simplest unifying models of this phenomenon is the twin-exhaust model (Blandford and Rees 1974, hereafter BR; Wiita 1978*a*, *b*). Here one assumes that a rotating gas cloud, in an external gravitational potential, has a point source of constant luminosity in its center. When this source turns on, it blows a bubble of hot gas. This bubble remains spherical until its radius reaches roughly one scale height of the confining gas cloud, at which time it rapidly burrows a tunnel along the path of least resistance—the rotational symmetry axis. The final state is then a double jet extending from a central cavity in the rotating cloud outward to large distances.

Although this model has been used a great deal, no detailed hydrodynamical calculation has been made to show that such a jet can indeed form and that it is hydrodynamically stable. Here we report the preliminary survey of a series of such calculations. We compare them with the steady state analytic work of BR and the dynamical calculations of the jet boundary by Wiita.

II. CALCULATION APPROACH

a) The Confining Cloud

The nature of confining gas cloud is largely determined by the gravitating mass distribution the gas is in. There are three basic cases of interest: (1) a self-gravitating gas cloud, (2) a gas cloud in an extended stellar cluster, and (3) a gas cloud bound by a point-mass potential such as a black hole. The first and second case yield a flat bottomed potential, while the third case yields a cusp (GM/r) potential. Because this latter case is dominated by the details near the black hole, we defer its consideration to a later paper.

Our calculation is a compromise between cases (1) and (2). We choose the gravitational potential to be that of a self-gravitating rotating cloud, but the gas dynamics are performed in that fixed potential, as if the potential were caused by a stellar background. We believe this approach is reasonable for discovering the nature of the nozzle formation and stability in any flat bottomed potential. We stress that the results in this paper are of a model hydrodynamic calculation. Astrophysical interpretations will be considered in later work.

The cloud has an equation of state given by $\gamma = \frac{5}{3}$. We used an initial density profile of the form:

$$\rho(R, Z) = \rho_0(1 + a\xi + b\xi^2)e^{-\xi} ,$$
$$\xi \equiv c(z^2 + d^2R^2)^{1/2} , \qquad (1)$$

where (R, Z) are cylindrical coordinates and $(a, b, c, d) = (1, 0.5, 15, 0.5)$. The profile (Fig. 1) is ad hoc and was selected to represent two major cloud characteristics: (1) a flat bottomed potential (a and b) and (2) a highly nonspherical (2:1 with $d = 0.5$) pressure distribution. The exponential atmosphere (c) was used so that the cloud would fit on the grid, not because we expect such atmospheres in astrophysical jet sources. Given the density profile (1), the angular momentum, pressure, and gravitational potential were solved for so that the cloud was in self-gravitating hydrostatic equilibrium. In general, neither P/ρ nor P/ρ^γ is constant, so the cloud is neither isothermal nor isentropic.

© American Astronomical Society • Provided by the NASA Astrophysics Data System

1981ApJ...247...52N

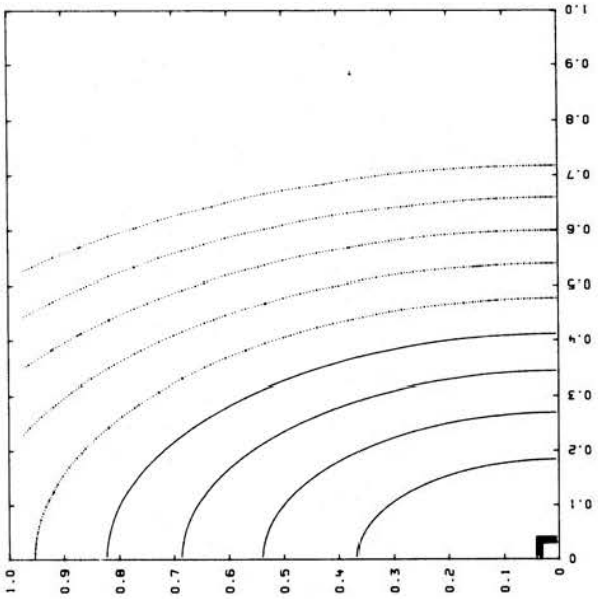


FIG. 1.—Density contours of the initial confining cloud (eq. [1]) for all calculations in this paper. The contours are spaced by a factor of 2. The vertical axis is the z-axis of rotational symmetry. The small square box in the center of the cloud is where the hot gas is introduced.

b) *The Numerical Method*

The hydrodynamic equations are solved by finite differencing, using a code developed for studying protostar formation (Norman, Wilson, and Barton 1979). One important feature of this code is that it can follow two gases with different equations of state independently, keeping track of the interface (or jet boundary) between them. Also the code has a careful treatment of angular momentum advection.

The initial hydrostatic cloud is solved for as stated above. Then hot light gas is continuously introduced into the central few (1–9) zones. This gas has specific internal energy $\epsilon_j = \delta\epsilon_c$, where ϵ_c is the central value of ϵ in the initial cloud and δ is a chosen constant ($\delta \sim 10$–100). The rate at which mass is introduced to the central zones is given by $\dot{m} = \partial_t m$, such that the central luminosity (L_c) source is constant in time:

$$L_c = \dot{m}\epsilon_j = \text{constant} . \quad (2)$$

The γ of this gas was chosen in different runs as $\frac{4}{3}$ or $\frac{5}{3}$. The hot light gas is then computed as a second fluid. A given grid zone can have a volume fraction of each fluid. No heating or cooling, other than by shocks or volume change, is included. The results in this paper are performed with nonrelativistic equations, although we are currently using a special relativistic version of the code.

We briefly remark on how our approach differs from earlier numerical studies. Several calculations have been made of the effects of point explosions in the nucleus (e.g., Sanders 1976; Mollenhoff 1976). We use a continuous injection of energy. Wiita (1978*a*, *b*) used a "$1\frac{1}{2}$" dimensional code which solved for the motion of the jet boundary in a fixed background. This method cannot follow the detailed flow pattern or allow for feedback of the expanding hot fluid on the cold confining cloud. His results were most complete for the bubble regime, but could not follow actual jet formation far enough to determine the shape or stability of the nozzle. Rayburn (1977) used a hydrodynamic code to study the early stages of jet formation. He reported that his runs were hampered by two major problems: (1) lack of grid spatial resolution (he used a 10×20 grid), and (2) he could not integrate past the time the head of the jet hit the edge of the grid. Our code solves both of these problems. Our grid has 8 times as many grid points (40×40), with (10×20) being inside the nozzle in the hot gas. Furthermore, we can integrate far past the point that the jet front leaves the grid and thus we can study nozzle formation and stability.

We scaled our units so that $\epsilon_c = G = 1$. The total mass of the cloud is M which sets the length scale so that $Z_{\max} = R_{\max} = 1$. All quantities reported in this paper are therefore given in units of ϵ_c, G, M. The scaling factors are: $GM\epsilon_c^{-1}$ for length, $GM\epsilon_c^{-3/2}$ for time, $\epsilon_c^{5/2}/G$ for luminosity, etc. The reader may find it more convenient to convert ϵ to the sound speed by using $c_s^2 = \gamma(\gamma - 1)\epsilon$. For instance, the characteristic luminosity $L_c \equiv \epsilon^{5/2}/G = [\gamma(\gamma - 1)]^{5/2}(c_s/c)^5 L_G$, where $L_G \equiv c^5/G = 3.63 \times 10^{59}$ ergs s^{-1}.

III. RESULTS

a) *Structure*

The structure of our steady state jets are quite different in detail from those discussed by BR and Wiita. Figure 2 illustrates a typical situation: $L = 0.5$ and $\delta = 10$. The central cavity, of radius $R_0 \approx 0.15$, is dominated by a quasi-spherical acceleration zone. The hot gas, which is introduced to the central four zones at zero velocity, builds up a central "hill" of pressure and density. As the new gas flows radially outward down the hill, it accelerates smoothly to supersonic velocities (here to a maximum Mach number of $M = 2$). This terminates at a radius $\sim 2R_0/3$ in a quasi-spherical shock front across which the velocity drops to subsonic. Collimation occurs immediately after shocking.

The subsonic gas then quickly accelerates down the z-axis until it reaches transonic velocity ($M = 1$) at a de Laval nozzle. Although this verifies the basic idea of BR, the dimensions of the nozzle are completely different from their original model. Wiita (1978*b*) states that the two necessary self-consistency conditions for a BR nozzle are $Z^* \gtrsim 3R_0$ and $Z^* \gtrsim 10R^*$, where Z^* is the location of the nozzle with radius R^*. This was necessary to guarantee the one-dimensional flow they assume in their calculations. In Figure 2 one sees that $R_0 = 0.15$, $R^* = 0.10$, $Z^* = 0.20$, and therefore $Z^* = 1.3R_0$ and $Z^* = 2R^*$, in contradiction to Wiita's and BR's assumptions. *Our cavity-nozzle structures are thus much more compact than BR's.* The reason for this is intimately coupled to the existence of the central shock.

Rees (1976, his Fig. 5) and Blandford (unpublished research notes) later realized that if a central shock

© American Astronomical Society • Provided by the NASA Astrophysics Data System

1981ApJ...247...52N

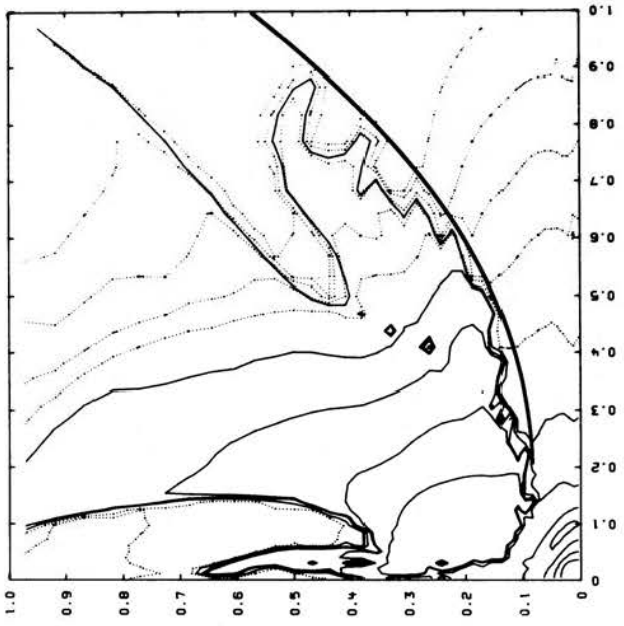


FIG. 2*a*

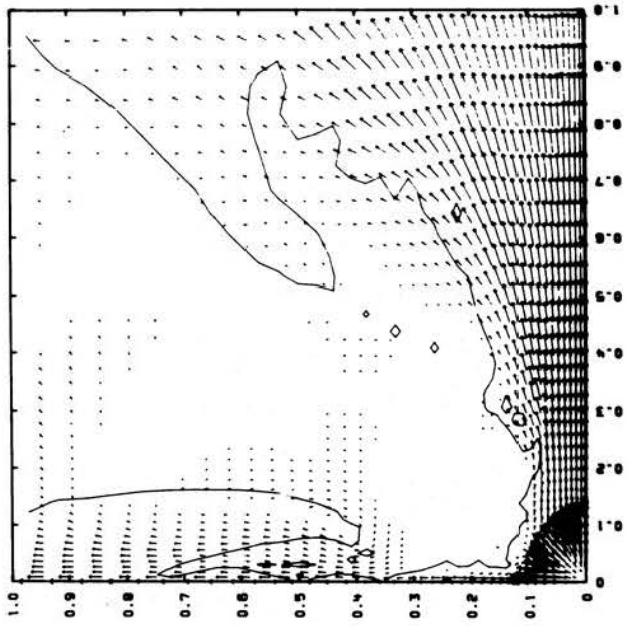


FIG. 2*b*

FIG. 2.—(*a*) Density contours of the cloud-jet structure at $t = 1.6$. The solid line is the predicted jet wall, while the closely spaced contours near this line is the computed jet boundary. (*b*) The velocity vector field at the same time as Fig. 2*a*. Notice the general features of central acceleration zone ending in a spherical shock. The radius of the shock is a large fraction of the radius of the cavity. The nozzle is at $z \approx 0.2$. A torus of hot gas has escaped along the equatorial plane.

formed, then the nozzle would have roughly the same radius as the shock. We present here the proof of this for a strong shock, following Blandford. If the central shock is strong, then the Mach number of the shocked gas in the cavity, M_c, is independent of the details of the flow before the shock:

$$M_c^2 = \gamma P_c/\rho_c V_c^2 = (\gamma - 1)/\gamma \,, \tag{3}$$

where $P = k\rho^\gamma$. This combined with Bernoulli's law neglecting gravity (see eq. [7] below) yields the nozzle velocity:

$$V_n = [(\gamma + 1)/(\gamma - 1)]^{1/2} V_c \,; \tag{4}$$

and the nozzle density:

$$\rho_n = [(\gamma + 1)/2\gamma]^{1/(\gamma - 1)} \rho_c \,. \tag{5}$$

These are finally combined with mass conservation, $\rho v A =$ constant, to obtain the area and therefore the radius of the nozzle:

$$r_n = 2^{1/2}[2\gamma/(\gamma + 1)]^{1/(2\gamma - 2)}[(\gamma + 1)/(\gamma - 1)]^{1/4} r_c \,. \tag{6}$$

For the case of $\gamma = \frac{4}{3}$ employed in Figure 2, we have $M_c = 0.5$, $V_n = 2.7 V_c$, $\rho_n = 0.67\rho_n$, and $r_n = 1.05 r_c$. We find numerically that the central shock is not quite a strong shock and therefore we have analyzed this more general case in a later paper. However, the basic results shown here are not altered.

Since the shock radius is $\sim 2R_0/3$, the nozzle radius must be a large fraction of the cavity radius, consistent with our calculations. If the central luminosity is decreased, the strength and radius of the shock will decrease and the cavity-nozzle structure begins to move toward the original BR structure. However, as we will see below in more detail, the nozzle becomes unstable to bubbling before the luminosity can be reduced enough to make a BR cavity-nozzle. In our lowest jet luminosity case $L = 0.05$, the shock has nearly disappeared and $Z^*/R^* \sim 4$, still much smaller than the $Z^*/R^* \gtrsim 10$ BR case.

We now examine how well our numerical calculations satisfy conservation laws. If we write the equation of state as $P = K\rho^\gamma$, then K specifies the entropy. The cool cloud has some initial $K(R, Z)$ specified by our manner of solving for the static configuration. The hot gas is introduced with a higher entropy (determined by $\delta = \epsilon_j/\epsilon_c$). As it flows outward, this K changes across the central shock. After this, K should stay fixed along a streamline unless it encounters further shocks. We find that in Figure 2 K is roughly constant ($K \sim 2.6$), for the first half of the jet ($Z < 0.5$). In the last half of the jet ($0.5 < Z < 1.0$), there are occasionally jumps in K with $2 < K < 3$. This is to be compared with a jump of 10 in K across the jet wall. It is not clear whether these are numerically induced or represent internal shock structure which we are not resolving (see, e.g., Chang and Chow 1974).

The assumption of a steady adiabatic flow, applied to the momentum equation, leads to Bernoulli's equation. For a γ-law gas in a fixed potential $\Phi(R, Z)$, we have (see, e.g., Courant and Friedrichs 1948):

$$C_* \equiv \left[\frac{\gamma - 1}{\gamma + 1}\right]^{1/2} \left[V^2 + \left(\frac{2}{\gamma - 1}\right) C_s^2 + 2\Phi\right]^{1/2} , \tag{7}$$

© American Astronomical Society • Provided by the NASA Astrophysics Data System

1981ApJ...247...52N

where C_*, the critical speed, is a constant. Our $\Phi = -2.75$ at the center, rises to -2.4 by $Z \approx 0.2$ (the nozzle location), and is -0.9 at $Z = 1$. At the nozzle $V = c_s = [\gamma(\gamma - 1)]^{1/2}\epsilon_n^{1/2}$. But $\epsilon_n = \delta\epsilon_{cn}$, where ϵ_{cn} is the specific internal energy of the external cloud at $Z = Z_n$. Thus, since we use the same cloud structure and same Φ for all L, we expect C_* is a function of δ only. This we find to be true with $C_* \approx 1.4$ for $\delta = 10$ and $C_* \approx 4.8$ for $\delta = 100$. Furthermore, C_* is quite constant down the axis and across the nozzle, suggesting that our final states have achieved steady adiabatic flow.

We find that the nozzle forms at roughly the distance where the pressure of the external cloud would have fallen by 2 from its central value if the hot gas had not pushed out the center of the cloud. This is $Z \approx 0.2$. However, the actual pressure drop from the shock to the nozzle is less than 2 since the velocity v of the hot gas does not fall to zero across the shock, and therefore equation (7) implies $C_s^2 = \gamma P/\rho$ must decrease by a smaller amount as $V \to C_s$.

We can use mass conservation to estimate the expected location of the jet wall. Since $\rho VA =$ constant, we can use (3) to rewrite the area of the jet $A \equiv \pi R_w^2$ as:

$$\bar{R}_w = \bar{\rho}^{-1/2}\bar{V}^{-1/2},$$

$$V = \left[\left(\frac{\gamma+1}{\gamma-1}\right)C_*^2 - \left(\frac{2}{\gamma-1}\right)C_s^2 - 2\Phi\right]^{1/2}, \quad (8)$$

where $\bar{R}_w = R_w/R_n$, $\bar{\rho} = \rho/\rho_n$, and $\bar{V} = V/C_{sn}$. The shape of the jet $\bar{R}_w(Z)$ in Figure 2 is dominated by $\bar{\rho}$ since $0.7 < \bar{V}^{-1/2} < 1.0$ along the jet, whereas $\bar{\rho} \approx 2.7e^{-5Z}$. Thus, the jet is an exponential horn and agrees well with the full hydrodynamic calculation. Notice that there is a cocoon of low-velocity hot gas outside of the jet boundary left over from the formation process.

Bernoulli's law (7) implies that as $z \to \infty$ and $C_s \to 0$, the velocity of the flow approaches a limit velocity $V_{\rm lim} \approx 2.65C_*$ (for $\gamma = \frac{4}{3}$) and an infinite Mach number. In Figure 2, $V_{\rm lim} \approx 4$ and at $Z = 1.0$ the velocity has reached $\sim 80\%$ of this limit velocity, while $M \approx 4.5$ there and is rising steeply.

Thus, we have approximately steady adiabatic flow in our jet. The energy input into the center is shared at finite radius between kinetic energy, internal energy, and gravitational energy. However, as the limit velocity is reached, only the kinetic energy of the jet contributes. Assuming the flow can be approximated by constant velocity $V_{\rm lim}$ across two jets of radius R, the luminosity should approach $L_{\rm lim} \approx \pi R^2\rho V^3 \approx \pi(\rho^* V^* R^{*2})V_{\rm lim}^2$, where mass conservation allows us to write ρVA as a constant. We find that $L_{\rm lim}/L \approx 1.0$ for all L as expected.

b) *Formation*

Although we cannot go into detail here, we will briefly describe the formation of the jet (Fig. 3), the early stages of which Wiita (1978*b*) studied. The interface between the two gases expands outward spherically until $Z \approx 0.10$, driving a spherical shock in front of it. After $Z \approx 0.10$ (note this is less than 1 scale height, $l \sim 0.17$), the interface along the z-axis begins to outpace the interface on the equator. Up until $Z \sim l$ the interface is decelerating, while after $Z \sim l$ it accelerates rapidly (see Shapiro 1979 on this point). The rate of acceleration increases with L. The interface hits $Z = 1.0$ at $t = 1.1$ for $L = 0.05$, whereas this occurs at $t = 0.3$ for $L = 2.0$. The deceleration-acceleration phases can be seen to occur in Wiita's calculations as well (e.g., by plotting his Fig. 4 linearly). After $Z \sim l$, the interface along the axis expands supersonically relative to the confining cloud while the interface along the equator moves outward subsonically. In Figure 2 one can see the subsequent formation of (1) the nozzle, (2) the "mushroom cloud" of hot gas surrounding the jet, and (3) an equatorial disk of hot gas (described below). All three of these features are still present at late times (Fig. 2).

None of the features are seen in Wiita's (1978*b*) Figure 5. However, this does not indicate his method has failed. His calculations all assume a relativistic fluid whereas the results we have discussed so far are for nonrelativistic fluids. However, we can conclude that the nozzle formation process exhibits more variety and instability than has heretofore been demonstrated.

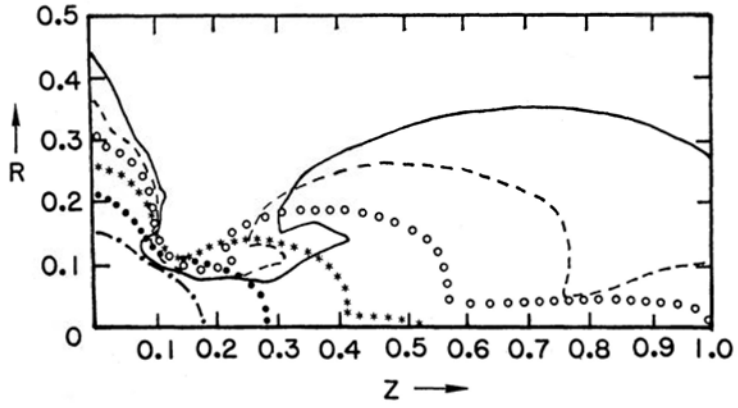


FIG. 3.—Locus of hot gas–cold gas interface (jet-cavity wall), for the $L = 0.5$ calculation, at different times: 0.18, 0.32, 0.45, 0.59, 0.72, 0.84. The wall at $t = 1.6$ is shown in Fig. 2. Notice the simultaneous formation of the cavity and nozzle.

© American Astronomical Society • Provided by the NASA Astrophysics Data System

1981ApJ...247...52N

c) *Stability*

We turn now to the stability of the jet structure which we divide into global and local stability. By global we refer to the overall structure of cavity-nozzle-jet. The primary consideration is whether a steady state is reached. To determine this, we integrate forward several oscillation periods $T_{osc} \approx 0.4$ of the cold cloud. As the cloud oscillates, the nozzle radius R^* oscillates as well. Note that we define T_{osc} as twice the sound crossing time for the inner region of the confining cloud $\sim 2lc_{sn}^{-1}$. The low-density outer regions have a much longer response time; therefore the final shape and stability of the outer part of the jet are not well studied in this calculation.

For $L \lesssim 2.0$ the structure seems to be stable. However, for $L = 2.0$ ($\delta = 100$) an instability occurs. First, a normal cavity-nozzle forms (Fig. 4 at $t = 0.68$). Note that the cavity and nozzle are much larger than for $L = 0.5$. As the cloud begins to oscillate inward, the cavity is so large that it forces the confining matter to flow toward the nozzle. What follows is a complicated Rayleigh-Taylor instability of the hot cavity (Fig. 5), leading to its fragmentation. It is almost impossible to numerically determine this disintegration. Indeed, with half the resolution (a grid of 20×20 instead of 40×40) this instability did not occur. It seems likely that after the fragmentation the nozzle may reexpand, producing an intermittent jet. For $L > 2.0$ the Rayleigh-Taylor instability is likely to be even more destructive, perhaps preventing high luminosity sources (relative to the cloud luminosity $\epsilon_c^{5/2}/G$) from forming jets.

A less fatal instability is seen both in Figures 2 and 3 ($L = 0.5$) and in Figure 4 ($L = 2.0$). This is the loss of a large portion of hot gas from the central cavity to form a large equatorial torus. We found this to occur quite often for the stronger ($L \geq 0.5$) sources. It did not occur for $L = 0.05$. This loss of gas occurs by a combination of Rayleigh-Taylor and Kelvin-Helmholtz modes which one can see beginning to pinch off at $t = 0.84$ in Figure 3. Whether this instability will periodically recur for moderate L we cannot yet say. However, in general one would suspect this stagnant ($v \approx 0$) point of the cavity to be rather unstable.

Finally, we come to the local or Kelvin-Helmholtz (K-H) stability of the nozzle and jet wall. While a number of authors (Blandford and Pringle 1976; Turland and Scheuer 1976; Ferrari, Trussoni, and Zaninetti 1978; Hardee 1979) have investigated linear perturbations of various idealized backgrounds, none of these studies were conclusive because they had to neglect the nonlinear terms which would determine the final state. Our difficulty is that we are limited by the finite grid size from seeing any but the largest wavelength ($\lambda \sim R^*$) instabilities. But these we do see. In Figure 1 one can see a typical situation. The ratio of velocities across the nozzle wall is ~ 10, so there is a strong shear present. Perturbations are generated on the wall of the central cavity; and as they grow in amplitude, they are swept out along the nozzle wall. The velocity of these bumps along the wall is roughly one-third of the jet velocity near the nozzle. Since the ratio of sound speeds across the wall is only $\sim \frac{1}{2}$, this means that the blobs move subsonically with respect to both the hot jets and cold cloud for our choice of $\delta = 10$.

Usually, these bumps simply make the wall ragged, but occasionally they pinch off from the confining cloud and become (toroidal) blobs in the jet. These dense blobs

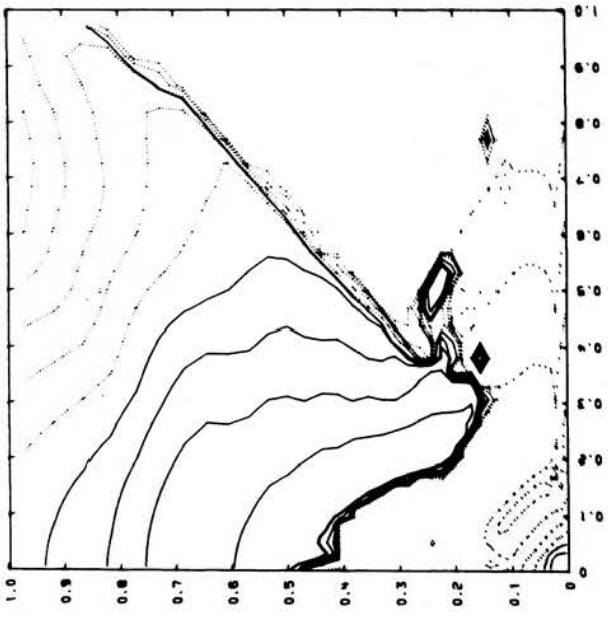


FIG. 4*a*

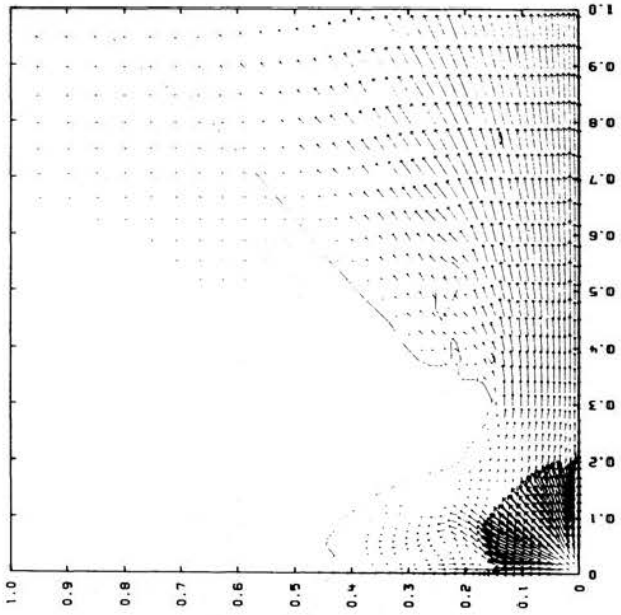


FIG. 4*b*

FIG. 4.—(*a*) Density contours of the $L = 2.0$ calculation at $t = 0.67$. (*b*) Velocity vector field for same time as Fig. 4*a*. Notice the beginning of a vortex in the cavity near the equator as well as a piece of wall breaking off then falling into the jet stream.

© American Astronomical Society • Provided by the NASA Astrophysics Data System

1981ApJ...247...52N

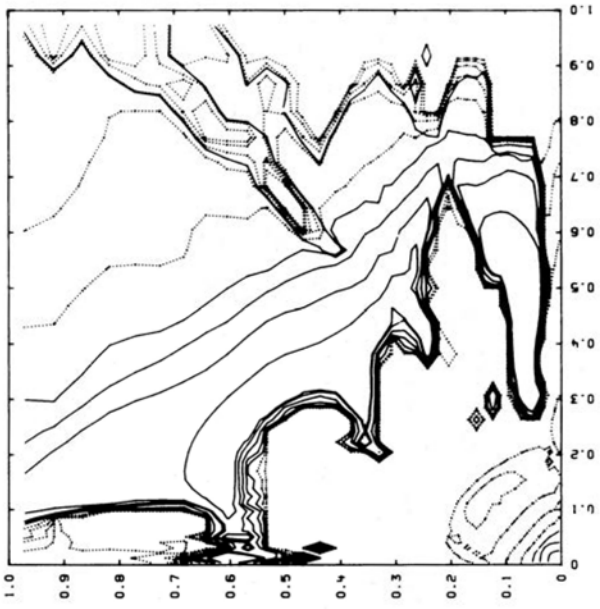


FIG. 5a

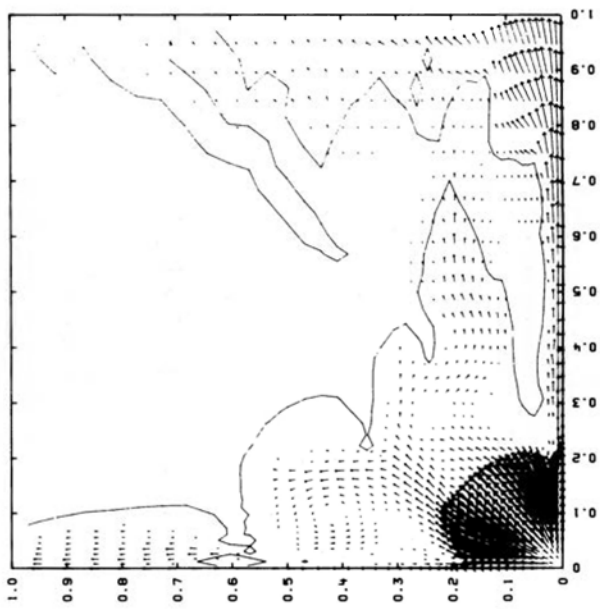


FIG. 5b

FIG. 5.—(*a*) Density contours of the $L = 2.0$ calculation at $t = 1.2$. Note the many density contours inside the "spike." The whole cavity has gone nonlinearly Rayleigh-Taylor unstable. (*b*) Velocity field for Fig. 5*a*. Notice how the nozzle has been nearly pinched off.

($\rho_{cl}/\rho_{jet} \sim 4.5$ in Fig. 2 at $Z \sim 0.2$) are slowly accelerated up to jet velocities and swept off the grid. This finite amplitude K-H instability at the nozzle may therefore be an important source of the clouds hypothesized, for instance, by Blandford and Königl (1979) to account for the knots in the M87 jet.

d) Luminosity Range

If the luminosity is low enough, the K-H instability will continually pinch off, producing a stream of bubbles (Smith *et al.* 1981). Wiita (1978*b*) also found that a lower limit to the luminosity exists because of bubble formation. However, we obtain a different range of values for L than he did. In order to compare with his work, we must convert his dimensionless luminosity $\mathscr{L}' \equiv L/(PC_s l^2)$ to our $L/(\epsilon_c{}^{5/2}G^{-1})$. This can be done quite generally by using $P = (\gamma - 1)\rho\epsilon$, $c_s{}^2 = \gamma(\gamma - 1)\epsilon$, and his definition of $l = (KT/\pi G\rho_s M_p)^{1/2}$. The result is:

$$\mathscr{L}' = \pi\mu^{-1}(\gamma - 1)^{-5/2}\gamma^{-1/2}[L/(\epsilon_c{}^{5/2}/G)] ,$$

where μ is the mean molecular weight of the gas. Using $\gamma = \frac{5}{3}$ and $\mu = \frac{1}{2}$, we have

$$\mathscr{L}' = 13.4[L/(\epsilon^{5/2}/G)] .$$

Our range in luminosity was between $L = 0.05\epsilon^{5/2}G^{-1}$ (bubbles) and $L = 2.0\epsilon^{5/2}G^{-1}$ (Rayleigh-Taylor unstable), corresponding to

$$0.67 < \mathscr{L}' < 26.8 .$$

For our shape ratio Wiita's $e = 0.96$. Looking at Wiita's (1978*b*) Figure 2, we see that our calculations have jets in his slow bubble and marginal regime. There are three major differences between our calculations and his which could explain the discrepancy: (1) his jets are relativistic, while ours are not; (2) his cloud pressure law is a pure exponential, not modified as in our equation (1); and (3) he assumed the pressure was uniform everywhere inside his jet boundary. We feel that the major difference is (3). Because of our central acceleration zone, the central pressure in our hot gas is much higher than the pressure near the head of the jet. This will act to prevent the neck from being cut off by the confining gas cloud as seen in Wiita's (1978*b*) Figures 6 and 7. That is, he chose his uniform pressure by dividing the total energy of the cavity by the volume. If this same energy has been arranged so that it had higher density (and therefore higher pressure) near the center, the cavity would be much stabler to forming bubbles. We remark that Wiita's assumption (3) was implied by his assumption (1) and therefore our nonrelativistic results do not indicate an error in his relativistic work.

There is an interesting new relationship which comes out of our analysis. We find that $L_j = \alpha\epsilon^{5/2}/G$, where $0.05 < \alpha < 2.0$. Converting ϵ to T for the case of thermal gas support $\gamma = \frac{5}{3}$ (ignoring radiation pressure), one finds

$$T = 5.7 \times 10^{-12}\alpha^{2/5}L_j{}^{2/5} .$$

That is, the value of the jet luminosity fixes the confining cloud temperature to within a factor of 4 ($0.3 < \alpha^{2/5} < 1.3$). In the opposite case of a self-gravitating gas cloud with radiation pressure support ($\gamma = \frac{4}{3}$), one finds that

$$L_j \approx \alpha(R_s/R)^{5/2}L_G ,$$

where $L_G = c^5/G = 3.6 \times 10^{59}$ ergs s^{-1}. Thus, in the radiation-supported case, the radius of the cloud compared to its Schwarzschild radius R_s is fixed. Both of

© American Astronomical Society • Provided by the NASA Astrophysics Data System

1981ApJ...247...52N

these constraints may lead to significant limitations on astrophysical models of jets. We stress that these formulae hold only for the flat bottomed potential we used (eq. [1]). The extension to other cases is the subject of a later paper.

IV. CONCLUSIONS

In conclusion, our numerical study has established the following points. First, a twin-exhaust de Laval nozzle can be formed hydrodynamically in a flat bottomed gravitational potential as envisioned by Blandford and Rees (1974). This nozzle is globally stable over a luminosity range of ~ 40, for a fixed confining gas pressure. For luminosities too low, the hot gas bubbles out, as described by Wiita (1979*b*), but for of luminosities too high the central cavity goes Rayleigh-Taylor unstable, fragmenting into hot clouds and destroying the nozzle. This behavior could lead to intermittent jets or to no jet at all. We find that the nozzles are short and compact, in contrast to the long nozzles envisioned by BR and Wiita (1978*a*). The nozzle is unstable to finite-amplitude Kelvin-Helmholtz, but not enough so that the nozzle structure is destroyed. Instead these K-H modes may pinch off and form cold dense blobs in the jets, thus providing an alternative source to the capture of clouds hypothesis of Blandford and Königl (1979). With an exponential falloff in density the jet shape expands outward exponentially, making such a density law unlikely to produce astrophysically interesting jets. We are currently investigating power-law falloffs'. Finally, we find a new relationship between the power of the jet and the properties (temperature or radius) of the confining cloud.

We would like to acknowledge useful conversations with R. D. Blandford, W. L. Chow, F. K. Lamb, J. Le Blanc, D. Lynden-Bell, J. A. Petterson, D. Pines, P. Shapiro, and P. J. Wiita. This work was partially supported by the Department of Energy and the National Science Foundation. One of us (L.S.) wishes to thank M. Rees for his stimulating discussions and hospitality at the Institute of Astronomy where this work was completed.

REFERENCES

Blandford, R. D., and Königl, A. 1979, *Ap. Letters*, **20**, 15.
Blandford, R. D., and Pringle, J. E. 1976, *M.N.R.A.S.*, **176**, 443.
Blandford, R. D., and Rees, M. J. 1974, *M.N.R.A.S.*, **169**, 395 (BR).
Chang, I.-S., and Chow, W. L. 1974, *AIAA J.*, **12**, 1079.
Courant, R., and Friedrichs, K. O. 1948, *Supersonic Flow and Shock Waves* (New York: Springer-Verlag).
Ferrari, A., Trussoni, E., and Zaninetti, L. 1978, *Astr. Ap.*, **66**, 43.
Hardee, P. E. 1979, *Ap. J.*, **234**, 47.
Mollenhoff, C. 1976, *Astr. Ap.*, **50**, 105.
Norman, M., Wilson, J., and Barton, R. 1980, preprint.
Rayburn, D. R. 1977, *M.N.R.A.S.*, **179**, 603.
Rees, M. J. 1976, in *The Physics of Non-Thermal Radio Sources*, ed. G. Setti (Dordrecht: Reidel).
Sanders, R. H. 1976, *Ap. J.*, **205**, 335.
Shapiro, P. 1979, *Ap. J.*, **233**, 831.
Smith, M. D., Smarr, L., Norman, M. L., and Wilson, J. R. 1981, preprint.
Turland, B. D., and Scheuer, P. A. G. 1976, *M.N.R.A.S.*, **176**, 421.
Wiita, P. J. 1978*a*, *Ap. J.*, **221**, 41.
———. 1978*b*, *Ap. J.*, **221**, 436.

MICHAEL L. NORMAN and JAMES R. WILSON: Lawrence Livermore Laboratory, University of California, Livermore, CA 94550

LARRY SMARR: Department of Astronomy, University of Illinois, Urbana, IL 61801

MICHAEL D. SMITH: Department of Physics, University of Illinois, Urbana, IL 61801

© American Astronomical Society • Provided by the NASA Astrophysics Data System